NPS-69-78-013

LEVEL

NAVAL POSTGRADUATE SCHOOL
Monterey, California

DEPARTMENT OF THE NAVY
NAVAL POSTGRADUATE SCHOOL

OCT 18 1978

Effects of Cavitation on Underwater

Shock Loading - Part 1

by

R. E. Newton

July 1978

78 10 06 017

NAVAL POSTGRADUATE SCHOOL
Monterey, California

Rear Admiral T. F. Dedman   Jack R. Borsting
Superintendent   Provost

Reproduction of all or part of this report is authorized.

This report was prepared by:
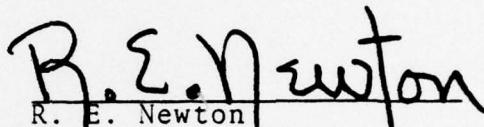
R. E. Newton
Professor of Mechanical Engineering

Reviewed by:
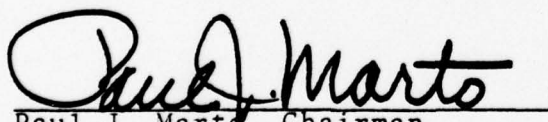
Paul J. Marto, Chairman   W. M. Tolles
Department of Mechanical   Dean of Research
   Engineering

REPORT DOCUMENTATION PAGE	READ INSTRUCTIONS BEFORE COMPLETING FORM

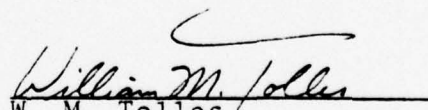| 1. REPORT NUMBER	2. GOVT ACCESSION NO.	3. RECIPIENT'S CATALOG NUMBER
NPS-69-78-013		

4. TITLE (and Subtitle)	5. TYPE OF REPORT & PERIOD COVERED
EFFECTS OF CAVITATION ON UNDERWATER SHOCK LOADING. PART 1.	Interim, April-June 1978
	6. PERFORMING ORG. REPORT NUMBER
	NPS-69-78-013

7. AUTHOR(s)	8. CONTRACT OR GRANT NUMBER(s)
R. E. NEWTON	MIPR-78-654

9. PERFORMING ORGANIZATION NAME AND ADDRESS	10. PROGRAM ELEMENT, PROJECT, TASK AREA & WORK UNIT NUMBERS
Naval Postgraduate School Monterey, CA 93940	Y99QAXSF501 Work Unit 16

11. CONTROLLING OFFICE NAME AND ADDRESS	12. REPORT DATE
Defense Nuclear Agency SPSS Washington, D. C. 20305	July 1978
	13. NUMBER OF PAGES

14. MONITORING AGENCY NAME & ADDRESS(if different from Controlling Office)	15. SECURITY CLASS. (of this report)
32p.	UNCLASSIFIED
	15a. DECLASSIFICATION/DOWNGRADING SCHEDULE

16. DISTRIBUTION STATEMENT (of this Report)

17. DISTRIBUTION STATEMENT (of the abstract entered in Block 20, if different from Report)

18. SUPPLEMENTARY NOTES

19. KEY WORDS (Continue on reverse side if necessary and identify by block number)

Underwater shock, shock mitigation, cavitation, finite elements.

20. ABSTRACT (Continue on reverse side if necessary and identify by block number)

Reported here are analytic formulations, together with one-dimensional results, in an investigation of the title subject. It is shown that either displacement or a displacement potential may be used as the basic dependent variable for a finite element analysis. Artificial damping is found to be needed to suppress spurious oscillations (a numerical phenomenon) near cavity boundaries. Adequacy of the method is demonstrated by comparison with published results of Bleich and Sandler. Some results are given for effects of cavitation on the performance of resilient attenuators.

DD FORM 1473   EDITION OF 1 NOV 65 IS OBSOLETE
1 JAN 73
S/N 0102-014-6601 |

TABLE OF CONTENTS

LIST OF FIGURES

1

EFFECTS OF CAVITATION ON UNDERWATER
SHOCK LOADINGS - Part I

Abstract

Reported here are analytic formulations, together with one-dimensional results, in an investigation of the title subject. It is shown that either displacement or a displacement potential may be used as the basic dependent variable for a finite element analysis. Artificial damping is found to be needed to suppress spurious oscillations (a numerical phenomenon) near cavity boundaries. Adequacy of the method is demonstrated by comparison with published results of Bleich and Sandler. Some results are given for effects of cavitation on the performance of resilient attenuators.

EFFECTS OF CAVITATION ON UNDERWATER
SHOCK LOADINGS - Part I

1. Introduction

1.1 <u>Earlier Work</u>. Motivation for the present investigation originated with the "shock shield" proposed by Geers in Ref. 1. The shield is a gas-filled cushion (GFC) to be fitted to the exterior of a submarine hull. If the cushion has sufficient thickness it can greatly reduce the magnitude of underwater shock loads transmitted to the hull. Related concepts involving the application of resilient elastic layers (REL) are treated by Geers in Ref. 2.

1.2 <u>Cavitation Effects</u>. The two-dimensional analyses of Refs. 1 and 2 neglect possible effects of cavitation. It is well-known (see Refs. 3 and 4), however, that a highly compliant submerged object will produce a negative pressure scattered wave in response to an incident shock wave. If the shock pressure is much greater than the hydrostatic pressure, cavitation will be induced in the fluid. Such cavitation may significantly increase the shock loading on the submerged body. It is thus evident that an adequate investigation of the effectiveness of resilient attenuators requires evaluation of effects of cavitation on performance.

1.3 <u>Plan for Investigation</u>. The present investigation is divided into two phases. The first phase is the subject of this report. It involves consideration of representative one-dimensional problems for the purpose of determining the relative merits of alternate choices for: dependent variables, time

3

integration algorithms, and spatial and temporal discretization.
The one-dimensional context allows rapid and inexpensive compu-
tations and allows comparison of results with those reported by
others. An account of this phase is given in the remaining
sections of this report.

The second phase of the investigation consists of extensions
to problems in three dimensions. Reasonable limitations on com-
puter core capacity and processing time require that the problems
be axisymmetric and, thus, mathematically two-dimensional.

1.4 <u>Fluid Model</u>. It is known that fluids do have some capacity
for sustaining negative pressure (tension). Some data are given
in Ref. 5. The influence of dissolved gas on the development
of cavitation is considered in Ref. 6. For the purpose of the
present investigation it is advantageous, and presumably con-
servative, to assume that the transition from the normal to the
cavitated state takes place without delay when the absolute
pressure reaches zero.

In the initial stages of this investigation the fluid was
treated as bilinear with a greatly reduced bulk modulus in the
negative pressure region. Subsequent developments disclosed
that the expected advantages of the bilinear model were not
achieved and the bulk modulus was henceforth assumed to be zero
in the cavitated region.

4

2. Choice of Dependent Variable

2.1 <u>Failure of the Pressure Formulation</u>. At the outset, this investigator expected that a formulation of the governing equations using fluid pressure p as the basic dependent variable would be advantageous. This expectation was based on previous successful finite element applications to propagation problems (e.g., see Refs. 7-9). Prior applications did not involve cavitation, but the bilinear fluid model was expected to handle successfully cavitation effects.

At an early stage of the investigation, duplication of the results of the example problem of Ref. 4 was attempted. These trials gave solutions which correctly tracked the growth of the cavitated region, but failed to show its subsequent contraction and collapse. Efforts to discover the reason for the failure of the pressure formulation led to a simple test problem which determines whether a proposed formulation can correctly track the contraction of a cavitated region. The problem is defined in the following section.

2.2 <u>"Water-Hammer" Problem.</u> The rapid pressure rise which accompanies the sudden interruption of water flow in a closed conduit is known as water-hammer. We here consider a flow in a zero pressure (or a small negative pressure, if the bilinear fluid model is used) cavitated region with positive dilatation e_0. Thus we have, for a semi-infinite region $x > 0$, the initial values:

$$p(x,0) = 0, \quad \text{(pressure)}$$
$$e(x,0) = e_0 > 0, \quad \text{(dilatation)}$$
$$\dot{u}(x,0) = -v_0 < 0. \quad \text{(velocity)}$$

The boundary condition at $x = 0$ is $\dot{u}(0,t) = 0$. The exact solution to this problem is especially simple. A shock front propagates with constant speed αc, beginning at the closed end, and the fluid behind the front is at rest with uniform pressure $p_1 = \alpha \rho c v_0$. Meanings of the symbols introduced are:

ρ = fluid density,

c = acoustic velocity.

Factor α is given by

$$\alpha = [1 + (ce_0/2v_0)^2]^{\frac{1}{2}} - (ce_0/2v_0).$$

In the region ahead of the shock front ($x > \alpha ct$) the variables p, $\dot{u}$, and e maintain their initial values.

2.3 <u>Governing Equations</u>. Details concerning the governing equations are given in Appendix A. Equations are stated in forms suitable for any number (i.e., one, two, or three) of spatial dimensions. Four separate formulations are developed with the principal dependent variable being particle displacement, fluid pressure, velocity potential, and displacement potential for the respective cases. The capability of each to deal with the one-dimensional water-hammer problem is discussed separately below.

2.4 <u>Displacement Formulation</u>. In this case it is convenient to replace the displacement vector $\underline{\delta}$ by $\underline{r} = \rho\underline{\delta}$ and, instead of the dilatation e, a density - weighted condensation $s = -\rho e$ is introduced. The working equations (Eqs. A11, A12, and A10) consist of an equation expressing $\underline{\ddot{r}}$ in terms of the gradient of p, one

6

giving s as the negative of the divergence of $\underline{r}$, and the pair of
algebraic relations for calculating p from s (the bilinear con-
stitutive law). It is readily seen that the initial conditions
of the water-hammer problem allow determination of the initial
values of $\underline{r}$ and $\underline{\dot{r}}$. The first may be deduced through spatial
integration of the constant initial dilatation e_0 and the second
is known from the given initial velocity $-v_0$. Given these
required initial values and the boundary condition at $x = 0$,
the working equations suffice to solve the problem.

The displacement vector is continuous, but both velocity
and pressure are discontinuous at the shock front. The pressure
discontinuity is not representable by the shape functions of the
finite element method. Accordingly there must be a finite
length interval over which both the pressure rise and particle
deceleration take place. The necessity for this compromise must
be considered a defect (but not a disqualifying one) of the dis-
placement formulation. A further disadvantage, not shared by
any of the other formulations is that the principal dependent
variable is a vector, not a scalar. In the axisymmetric appli-
cations planned this will double the order and bandwidth of the
stiffness matrix, resulting in a great increase in requirements
for computer storage and processing time.

2.5 Pressure Formulation. In Appendix A the pressure formulation
is stated in terms of a second order equation (A 13) expressing
$\ddot{s}$ as the Laplacian of the dynamic component of pressure, together
with the bilinear constitutive relation (A 10). The solution
technique involves stepwise time integration for s, alternating

7

with use of the constitutive relation to find new values of p.
In view of the role played by s, it is slightly misleading to
call this the pressure formulation. Indeed, in the absence of
cavitation it is advantageous to use the constitutive relation
to eliminate s in favor of p alone. In cavitated regions, how-
ever, retaining s makes the strategem of a nonzero bulk modulus
unnecessary. Despite this advantage, both versions fail.

The reason this technique fails when applied to the water-
hammer problem is readily apparent. The variable s (and also p)
has a step discontinuity at the shock front. (Correspondingly,
the second derivative $\ddot{s}$ has a dipole singularity.) We know
that the height of the step depends on the initial (negative)
value of s and on the fluid velocity. The velocity, however,
is neither explicitly nor implicitly represented in the equations.
There seems to be no further reason to consider the pressure
formulation for cavitation problems.

The bilinear fluid model with a nonvanishing bulk modulus
in the tension region was initially introduced with the expec-
tation that the pressure formulation would work. Since the
sole reason for including this complication has vanished, we
shall henceforth exclude negative pressures and correspondingly
choose $\beta = 0$ in (A2), (A4), and (A10).

2.6 <u>Velocity Potential Formulation</u>. Using ϕ to represent the
velocity potential, the governing equations express $\dot{\phi}$ as the
negative of the dynamic pressure (A14), $\dot{s}$ as the negative of the
Laplacian of ϕ (A15), and p in terms of s (A10). In this

instance the velocity potential is continuous, but its first derivatives are not. It is possible to obtain a moderately satisfactory solution from the discretized equations.

2.7 Displacement Potential Formulation. Using ψ to represent the displacement potential, the governing equations express $\ddot{\psi}$ as the negative of the dynamic pressure (A16), s as the negative of the Laplacian of ψ (A17), and p in terms of s (A10). All of the needed variables appear, explicitly or implicitly, in this formulation. Moreover, ψ and its first derivatives are continuous. The step discontinuities in p, s, and $\dot{u}$ are manifested as discontinuities in the second derivatives of ψ.

2.8 Formulation Selection. Among the formulations considered, the pressure-based one is discarded as unworkable and the velocity potential is rejected as inferior to the displacement potential on the basis of continuity. In the remainder of this report, discussion of application details will be confined to the ψ formulation because it is novel. The displacement formulation was developed in parallel and also tested on the Bleich-Sandler example (Ref. 4).

2.9 Discretized Equations and Solution Process. The process of forming discretized finite element equations from the corresponding partial differential equation is well known (e.g., see Ref. 7) and will not be repeated here. We note that, based on prior experience with wave propagation problems, linear shape functions were chosen. It was found that a lumped "mass" matrix was easier to use and gave better performance than its consistent counterpart.

9

Details concerning the formulation of initial conditions
and the radiation boundary condition are given in Appendix B.
The considerations used for selecting a time integration algor-
ithm and the means for introducing needed artificial damping
are discussed in Appendix C.

3. The Bleich-Sandler Example

3.1 Statement of the Problem. In Ref. 4 Bleich and Sandler,
using a bilinear fluid model, study cavitation phenomena during
one-dimensional wave propagation. They use the method of
characteristics and introduce additional relations to connect
state variables on opposite sides of a shock front.

The numerical example they give concerns "the response of a
horizontal layer of mass on the surface of a half-space of fluid,
Fig. 1. A plane pressure wave with a sudden rise and an expon-
ential decay moves toward the surface, reaching the mass at the
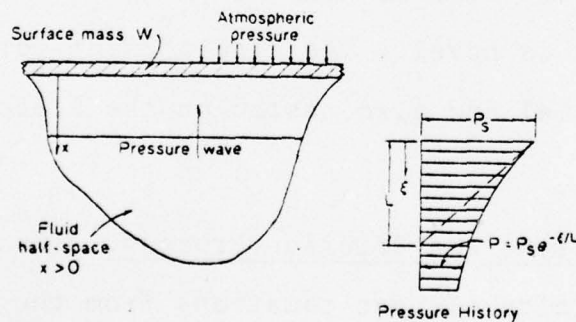
Figure 1. Particulars of Bleich-Sandler example (from Ref. 4).

time t = 0. The system is subject to gravity and atmospheric
pressure, all particles being at rest prior to arrival of the
shock. The analysis is based on the degenerate model with β = 0."

10

For calculation and presentation of results Bleich and Sandler use the time constant of pressure wave decay ($\approx$ 1 ms) as the time unit. The acoustic velocity c is given the convenient value unity by choosing unit length to be the distance traveled by the pressure wave in unit time ($\approx$ 56 in.).

3.2 Comparisons with Bleich-Sandler Results. Bleich and Sandler present two figures summarizing their solution. First of these traces the time history of the cavitated region in the x - t plane. Their figure is reproduced in Figs. 2 and 3 below with superposed points obtained by present analyses. For the finite element analyses the discretized region extends from x = 0 to a radiation boundary at x = 4. Results shown in Fig. 2
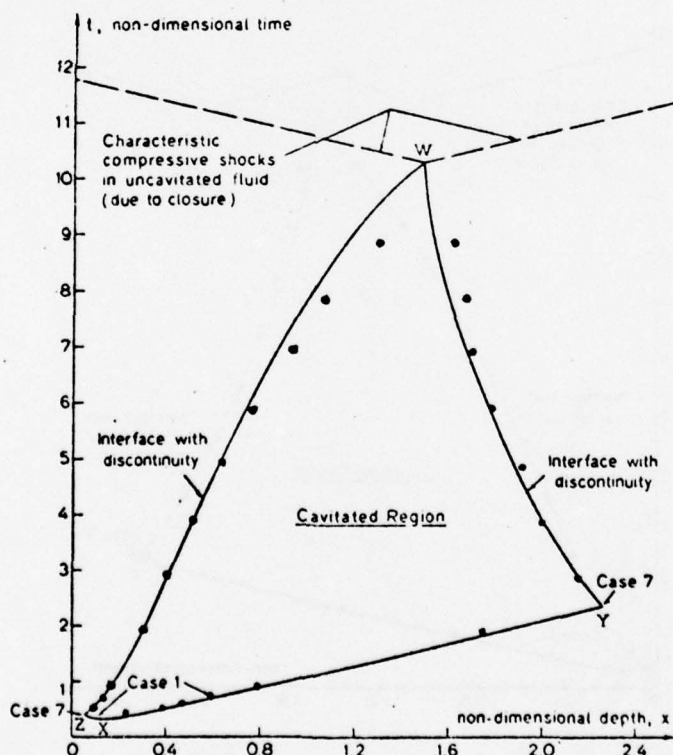
Figure 2. Bleich-Sandler example: time-history of the cavitated region. Discrete points found by finite element method using the displacement formulation.

11

were obtained from the displacement formulation using a node spacing (element length) $\Delta x = .04$ and a time step $h = .01$. In the absence of damping it was found that moving "islands" of positive pressure appeared within the cavitated region. This behavior is henceforth called "frothing." It was found that damping with $\eta = .16$ was sufficient to supress frothing and produce a smooth variation of the condensation s within the cavitated region.

In Fig. 3 the superposed points were obtained using the displacement potential formulation. For these results: $\Delta x = .01$
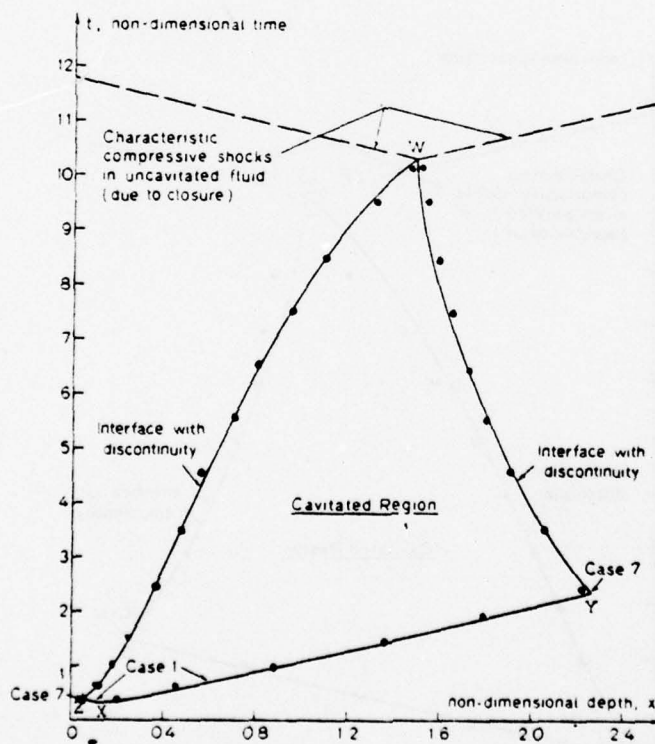
Figure 3. Bleich-Sandler example: time-history of the cavitated region. Discrete points found by finite element method using the displacement potential formulation.

12

and h = .0025. To suppress frothing a value η = .0025 was
found to be sufficient.

A second Bleich-Sandler figure shows the time history of
the velocity of the surface mass layer. This is reproduced as
Figs. 4 and 5. Points obtained from present analysis using the
displacement formulation are superposed on Fig. 4 and points
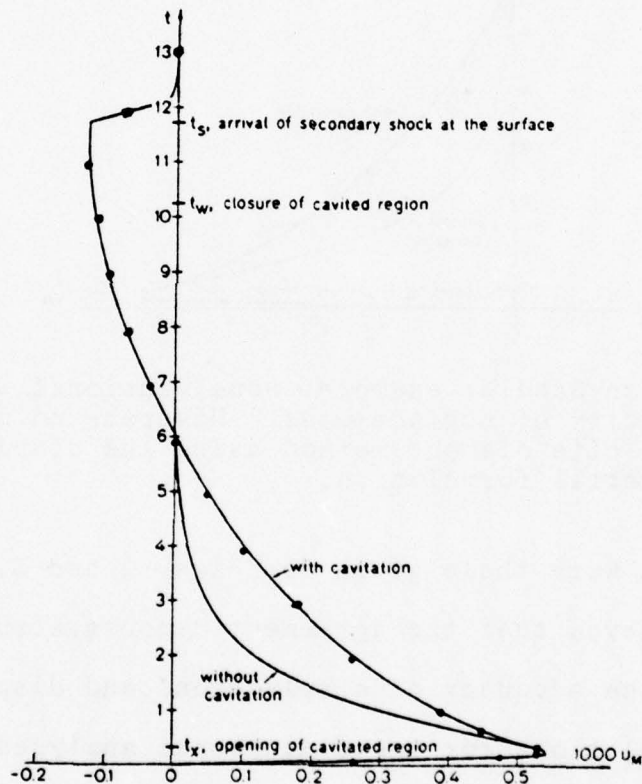
Figure 4. Bleich-Sandler example: nondimensional upward velocity
of surface mass. Discrete points found by finite
element method using the displacement formulation.

from the displacement potential formulation on Fig. 5, The

13
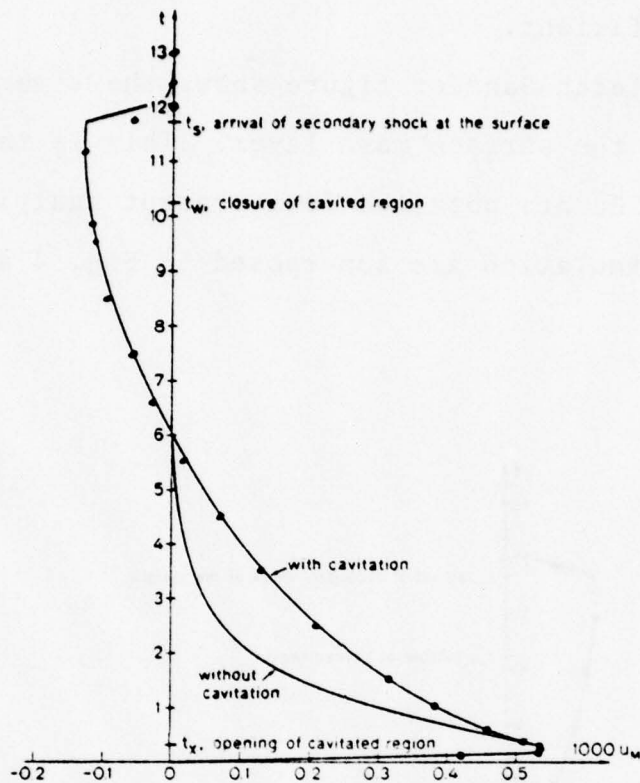
Figure 5.   Bleich-Sandler example: nondimensional upward
            velocity of surface mass. Discrete points found
            by finite element method using the displacement
            potential formulation.

parameters used were those given for Figs. 2 and 3, respectively.

    It is believed that the agreement demonstrated in Figs. 2-5

substantiates the adequacy of displacement and displacement

potential formulations for one-dimensional analyses.

14

4. Effect of Cavitation on Resilient Attenuator Performance

We consider here the effect of cavitation on the performance of two selected attenuators. One is a GFC with an initial thickness of 10 in. under hydrostatic pressure. The second is an REL with modulus C_1 = 1000 psi. and an initial thickness L_o = 10 in. when loaded only by atmospheric pressure[*]. The shock loading consists of a pressure step of amount p_s followed by exponential decay with time constant 25 ms. The hydrostatic pressure is p_h. Results are given as the quotient of the maximum dynamic pressure increment Δp_{max} by the peak shock pressure p_s.

If cavitation effects are ignored the response may be found by integrating numerically a first order ordinary differential equation. Details are omitted here.

The response considering cavitation has been determined using finite element modelling based on the displacement potential formulation. Results are summarized in Table 1.

Table 1. Effect of Cavitation on Attenuator Response

		Values of $\Delta p_{max}/p_s$			
p_h	p_s	GFC		REL	
psia	psia	N.C.[*]	W.C.[**]	N.C.	W.C.
30	1000	0.21	0.69	0.71	0.76
280	750	0.44	0.45	0.82	0.82

*N.C. = no cavitation   **W.C. = with cavitation

---

[*]It is postulated that the relation between gage pressure p_g and thickness L is $p_g = C_1(L_o/L-1)$.

Results in Table 1 show that cavitation has little effect on the performance of the REL considered at either hydrostatic pressure. This is also true for the GFC at p_h = 280 psi., but there is severe performance degradation at p_h = 30 psia. Note, however, that performance remains better than that of the REL. If the hydrostatic pressure is increased significantly above 280 psia., maintaining the relation $p_h + p_s$ = const., cavitation will not occur.

5. Conclusions

Both the displacement formulation and the displacement potential formulation have been shown to produce acceptable results when applied to the Bleich-Sandler example. It is anticipated that either formulation will provide a workable basis for solving three-dimensional axisymmetric problems. The scalar displacement potential will lead to a much smaller computer storage requirement and processing time, but it may not be easy to fit it to the framework of an existing program such as NASTRAN, MARC, or NONSAP. No insurmountable difficulty is anticipated in using the displacement formulation with one of these programs.

Appendix A. Governing Equations

Equations are derived here in a form independent of the number of spatial dimensions.

Newton's Second Law: $\rho\underline{\ddot{\delta}} = -\underline{\nabla}p + \underline{f}.$ 　　　　　　(A1)

In the above:

ρ　=　fluid density;

$\underline{\delta}$　=　particle displacement vector;

$\underline{\nabla}$　=　gradient operator;

p　=　fluid absolute pressure;

$\underline{f}$　=　body force per unit volume.

Note that the underline is used to denote a vector quantity. Differentiation with respect to time is denoted by a superior dot and the convective contributions to the material derivative are neglected.

Bilinear Constitutive Law:　$p = -c^2\rho e,\ e \leq 0;$

$$p = -\beta^2 c^2 \rho e,\ e > 0.$$ 　　(A2)

Here:

c　=　acoustic velocity in fluid;

e　=　dilatation.

Note that $c^2\rho$ is the bulk modulus of the fluid. For the bilinear fluid model β is chosen as positive and small compared with unity. The limiting condition of zero pressure in the cavitated region corresponds to $\beta = 0$.

Geometric identity:　$e = \underline{\nabla}\cdot\underline{\delta}$, 　　　　(A3)

where the dot denotes the scalar product.

It is possible to choose a single dependent variable such as p and, through suitably chosen manipulations, demonstrate that p obeys the wave equation in the uncavitated fluid and a modified form with βc in place of c in the cavitated region(s). Thus

$$\ddot{p} = c^2 \nabla^2 p, \quad p \geq 0;$$
$$\ddot{p} = \beta^2 c^2 \nabla^2 p, \quad p < 0. \tag{A4}$$

A more enlightening approach which focuses attention on the sequential steps in time integration of the governing equations uses auxiliary dependent variables and a set of three equations. For this purpose we first define some additional dependent variables and then summarize four separate formulations.

Definitions. In our applications the body force $\underline{f}$ appearing in (A1) may be expressed as

$$\underline{f} = \nabla p_h , \tag{A5}$$

where p_h is the hydrostatic component of fluid pressure.

It is useful to introduce two density weighted variables:

$$\underline{r} = \rho \underline{\delta} , \tag{A6}$$
$$s = -\rho e. \tag{A7}$$

We also introduce two similarly weighted potential functions:

$$\nabla \phi = \dot{\underline{r}}, \tag{A8}$$
$$\nabla \psi = \underline{r}. \tag{A9}$$

Henceforth we omit explicit reference to the density factor and refer to $\underline{r}$ as displacement, s as condensation (Lamb's usage,

18

see Ref. 10), ϕ as velocity potential and ψ as displacement potential.

Using s, the bilinear constitutive law is rewritten as

$$p = c^2 s, \qquad s \geq 0;$$
$$p = \beta^2 c^2 s, \qquad s < 0. \tag{A10}$$

In the computational stage a further simplification is effected by choosing length and time units such that $c = 1$.

r Formulation. Using (A5) and (A6), (A1) becomes

$$\ddot{\underline{r}} = -\underline{\nabla}(p-p_h). \tag{A11}$$

Using also (A7), (A3) becomes

$$s = -\underline{\nabla}\cdot\underline{r}. \tag{A12}$$

When applicable initial and boundary conditions are prescribed, the $\underline{r}$ formulation allows the following calculation sequence:

1. Using present values of p and p_h, calculate $\ddot{\underline{r}}$ from (A11).

2. Using a suitable time integration algorithm and the current values of $\underline{r}$ and $\dot{\underline{r}}$, find new values of $\underline{r}$ and $\dot{\underline{r}}$ after one time step.

3. Use (A12) to find new values of s.

4. Find corresponding new values of p from (A10).

5. Return to Step 1 with new values of p and repeat the sequence as many times as needed.

p Formulation. Determining the divergence of both sides of (A11), then calculating the second time derivative of each side of (A12) and substituting in the preceding result gives

$$\ddot{s} = \nabla^2(p-p_h). \tag{A13}$$

19

It appears as if a sequential use of (A13) and (A10) in a fashion paralleling that described above for the r formulation would allow tracking the time history of p. The process is workable in the absence of cavitation and has been successfully applied to a variety of problems (e.g., see Refs. 7-9). In such applications the variable s is superfluous and the first of (A4) suffices. Reasons for the failure of this formulation in a cavitated region are discussed in Art. 2.5.

ϕ Formulation. Using (A8) and (A11) we may deduce the result

$$\dot{\phi} = p_h - p. \tag{A14}$$

Further, using (A8) and (A12), we may find

$$\dot{s} = -\nabla^2 \phi. \tag{A15}$$

These two equations, followed by (A10), may be employed sequentially and repetitively to construct a time marching solution. Although ϕ, like p, satisfies the wave equation (A4), such a reduction of the equations still requires calculation of s by integrating (A15) to distinguish cavitated regions.

ψ Formulation. Using (A8) and (A9) we may transform (A14) into

$$\ddot{\psi} = p_h - p, \tag{A16}$$

and transform (A15) into

$$s = -\nabla^2 \psi. \tag{A17}$$

These two equations, followed by (A10), also may be used sequentially and repetitively to find the time history of p.

20

Appendix B. Initial and Boundary Conditions

Initial Values of ψ and $\dot{\psi}$. Considered here are the initial conditions for an uncavitated region with hydrostatic pressure p_h and a dynamic pressure p_{in} resulting from a wave travelling in the negative x direction. Thus, at time t:

$$p(x,t) = p_h(x) + p_{in}(x,t). \tag{B1}$$

Our immediate concern is with conditions at t = 0. Now

$$\psi_{,xx} = \rho \partial u/\partial x = -p(x,0)/c^2. \tag{B2}$$

Integrating twice gives the result

$$\psi(x,0) = \rho x u(0,0) - \frac{1}{c^2} \int_0^x \int_0^\lambda p(\zeta,0) d\zeta d\lambda, \tag{B3}$$

where the choice $\psi(0,0) = 0$ is arbitrary. For evaluation of $\dot{\psi}(x,0)$ we begin with

$$\dot{\psi}_{,x} = \rho \dot{u}. \tag{B4}$$

The particle velocity is induced by the incoming wave and is given by

$$\rho \dot{u} = -p_{in}(x,t)/c. \tag{B5}$$

Substituting (B5) into (B4) and integrating:

$$\dot{\psi}(x,0) = \rho c u(0,0) - \frac{1}{c} \int_0^x p_{in}(\zeta,0) d\zeta. \tag{B6}$$

The choice of $\dot{\psi}(0,0) = \rho c u(0,0)$ is useful in connection with the radiation boundary condition considered in the next article.

21

The initial conditions given by (B3) and (B6) are based on an incoming pressure wave in uncavitated fluid. The modifications required to deduce initial conditions for the water-hammer problem are obvious and are not detailed here.

Radiation Boundary Condition. Representation of a semi-infinite region by the finite element method requires some strategem for truncating the discretized region. The device employed here is an extension of the radiation boundary condition originally introduced in Ref. 7 and successfully employed in Refs. 8 and 9. The relations used are based on the d'Alembert solution to the wave equation. Thus, for an incoming wave:

$$\psi_{in}(x,t) = f(x+ct). \tag{B7}$$

Similarly, for an outgoing wave:

$$\psi_{out}(x,t) = g(x-ct). \tag{B8}$$

For our problems we may write

$$\psi = \psi_h + \psi_{in} + \psi_{out}, \tag{B9}$$

where ψ_h is contributed by the hydrostatic pressure. If we choose to terminate the region at $x = x_r$ (the radiation boundary), we require $\psi_{,x}(x_r,t)$ for our boundary condition. Using (B7), (B8), and (B9) it is readily established that

$$\psi_{,x} = \psi_{h,x} + 2\psi_{in,x} - \dot{\psi}/c. \tag{B10}$$

By rather obvious extensions of the manipulations leading to (B3), the needed values of $\psi_{h,x}$ and $\psi_{in,x}$ may be found. The value of $\dot{\psi}$ is generated in the solution process.

Appendix C.   Time Integration and Artificial Damping

Time Integration Algorithm.   Prior experience with transient
wave propagation studies by the finite element method (e.g.,
see Ref. 11) established the desirability of using a time
integration algorithm which effectively introduces damping that
increases with modal frequency.   Also desirable was a method
explicitly designed for second-order equations.   Two methods
known to meet these requirements are the Houbolt method (Ref. 12)
and the Wilson θ method (Ref. 13).   Both of these algorithms
can be unconditionally stable.   The Houbolt method introduces
greater spurious damping than Wilson's (Ref. 14).   This advan-
tage is offset by the fact that the Houbolt method approximates
the second time derivative by fitting a cubic polynomial to
four equally spaced ordinates.   Because of the discontinuities
inherent in the cavitation problem the Wilson method, which
utilizes only two adjacent ordinates for each time step, was
chosen.

The nonlinearity of the governing equations in the neigh-
borhood of a cavity boundary necessitates a nonstandard appli-
cation of the Wilson method.   Using θ = 1.4 the method assumes
that $\ddot{\psi}$ is a linear function of time from the current instant
for a duration 1.4h, where h is the time step.   For this appli-
cation, an initial estimate of the forward value of $\ddot{\psi}$ was based
on linear extrapolation.   The estimate was improved by iteration
before proceeding to the following time step.   An effect of
using this strategem was to introduce a limit on the maximum
usable time step (i.e., to sacrifice unconditional stability).

23

Artificial Damping. Initial solutions using the Wilson method

showed both temporal and spatial oscillations of pressure fol-

lowing passage of the shock front in the water-hammer problem.

Since no such behavior is shown by the exact solution, it is

clearly a numerical artifact. To suppress the unwanted oscil-

lation, damping was introduced into the governing equations.

The mechanism chosen was to modify (A16) to read

$$\ddot{\psi} = p_h - p - \eta \dot{s}. \tag{C1}$$

The coefficient η appearing in (C1) was chosen by cut-and-try.

The needed value of $\dot{s}$ is calculated from (A17) by differentiat-

ing with respect to time.

24

REFERENCES

1. Geers, Thomas L., "A Shock Shield Analysis, "LSMC-D558128, Lockheed Palo Alto Research Laboratory, March 1977.

2. Geers, Thomas L., "Shock-Wave Attenuation by Resilient Scatters," Journal of Applied Mechanics, Vol. 42, p. 390, 1975.

3. Temperley, H. N. V., "Theoretical Investigation of Cavitation Phenomena Occurring when an Underwater Pressure Pulse is Incident on a Yielding Surface," Underwater Explosion Research, Vol. 3, p. 255, 1950.

4. Bleich, H. H., and I. S. Sandler, "Interaction between Structures and Bilinear Fluids," International Journal of Solids and Structures, Vol. 6, p. 617, 1970.

5. Clay, C. S., and H. Medwin, Acoustical Oceanography; Principles and Applications, Wiley, 1977.

6. Kedrinskii, V. K., "Dynamics of the Cavitation Zone During an Underwater Explosion Near a Free Surface," Zh. Prikl. Mekh. and Tekh. Fiz. (USSR), No. 5, p. 68, Sept-Oct 1975.

7. Zienkiewicz, O. C., and R. E. Newton, "Coupled Vibrations of a Structure Submerged in a Compressible Fluid," In Finite Element Techniques, edited by M. Sorensen, University of Stuttgart, Germany, p. 359, 1969.

8. Dean, D. V., "Finite Element Study of Acoustic Waves," Thesis, Naval Postgraduate School, 1970.

9. Newton, R. E., and D. L. Atchison, "Response of a Ring-Stiffened Cylinder to an Acoustic Blast Wave," Proceedings, Second International Symposium on Finite Element Methods in Flow Problems, Santa Margherita Ligure, Italy, p. 703, June 1976.

10. Lamb, H., Hydrodynamics, Dover, p. 476, 1945.

11. Atchison, D. L., "Finite Element Solution of the Interaction of a Plane Acoustic Blast Wave and a Cylindric Structure," Thesis, Naval Postgraduate School, June 1974.

12. Houbolt, J. C., "A Recurrence Matrix Solution for the Dynamic Response of Elastic Aircraft," Journal of the Aeronautical Sciences, Vol. 17, No. 9, p. 540, September 1950.

13. Bathe, K. J., and E. L. Wilson, Numerical Methods in Finite Element Analysis, Prentice-Hall, p. 349, 1976.

14. Geradin, M., "A Classification and Discussion of Integra-
        tion Operators for Transient Structural Analysis,"
        in Finite Element Methods in Structural Dynamics,
        edited by T. H. H. Pian, AIAA Selected Reprint Series,
        Vol. XVII, 1974.

INITIAL DISTRIBUTION LIST

Copies

1. Defense Documentation Center   2
   Cameron Station
   Alexandria, Virginia 22314

2. Research Administration, Code 012A   1
   Naval Postgraduate School
   Monterey, California 93940

3. Professor R. E. Newton   4
   Mechanical Engineering Dept.
   Code 69Ne
   Naval Postgraduate School
   Monterey, California 93940

4. Pacifica Technology   1
   P. O. Box 148
   Del Mar, CA 92014

5. Columbia University   1
   Department of Civil Engineering
   S. W. Mudd Building
   New York, NY 10027
   ATTN: F. Dimaggio

6. Office of Naval Research
   Arlington, VA 22217
   ATTN: Code 715 (Tech Lib)   1
         Code 474 (Nicholas Perrone)   1

7. Weidlinger Associates
   Consulting Engineers
   110 East 59th Street
   New York, NY 10022
   ATTN: Melvin Baron   1
          D. Ranlet   1

8. Officer-in-Charge
   Civil Engineering Laboratory
   Naval Construction Battalion Center
   Port Hueneme, CA 93041
   ATTN: Code L08A (Library)   1

9. Commander
   Naval Ship Engineering Center
   Department of the Navy
   Washington, D. C. 20362
   ATTN: NSEC 6105   3
           Code 09G3 (Tech Lib)   1
           NSEC 6120D   1

10. Commander
    Naval Surface Weapons Center
    Dahlgren Laboratory
    Dahlgren, VA 22448
    ATTN: Tech Lib & Info Servs Brnch   1

11. Lockheed Missiles and Space Company, Inc.
    Palo Alto, CA 94304
    ATTN: Tom Geers D/52-33   1
            Bldg 205

12. General Dynamics Corporation
    Electric Boat Division
    Eastern Point Road
    Groton, CT 06340
    ATTN: V. Godino   1

13. SRI International
    333 Ravenswood Aven
    Menlo Park, CA 94025
    ATTN: George Abrahamson   1

14. Director
    U. S. Army Engineer
    Waterways Experiment Station
    P. O. Box 631
    Vicksburg, MS 39180
    ATTN: Library (Uncl only)   1
            John N. Strange   1

15. Commander
    David W. Taylor Naval Ship R&D Center
    Bethesda, MD 20084
    ATTN: Code 177   2
            Code 174   1
            Code L42-3 (Library)   1
            Code 2740 (Y.Wang)   1
            Code 1740.5   1

16. Officer-in-Charge
    Naval Surface Weapons Center
    White Oak, Silver Spring, MD 20910
    ATTN: Code CR-14 (Blatstein)   1

17. Commander
    Naval Weapons Center
    China Lake, CA 93555
    ATTN: Code 533 (Tech Lib)   1

18. Commander
    Naval Ocean Systems Center
    San Diego, CA 92152
    ATTN: Code 4471 (Tech Lib)   1

19. Director
    Naval Research Laboratory
    Washington, D. C. 20375
    ATTN: Code 2627 Tech Lib   1
          Code 8440 G. O'Hara   2

20. Director
    Defense Nuclear Agnecy
    Washington, D. C.
    ATTN: SPSS   6

21. Undersecretary of Defense for Research
        and Engineering
    Department of Defense
    Washington, D. C. 20301
    ATTN: Strategic & Space Systems (OS)   1

22. Headquarters
    Naval Material Command
    Washington, D. C. 20360
    ATTN: MAT 0323   1

23. Superintendent (Code 1424)
    Naval Postgraduate School
    Monterey, CA 93940
    ATTN: Code 2124 Tech Rpts Lib   2

24. Commander
    Naval Sea Systems Command
    Department of the Navy
    Washington, D. C. 20362
    ATTN: ORD-91313 (Lib)   1

25. Commander
    Field Command
    Defense Nuclear Agency
    Kirtland AFB, NM 87115
    ATTN: FCPR   1

26. Chief
    Livermore Division Fld Command
    Defense Nuclear Agency
    Lawrence Livermore Laboratory
    P. O. Box 808
    Livermore, CA 94550
    ATTN: FCPRL   1